Scientific
Research
Publishing

Fe₃O₄ and Fe Nanoparticles by Chemical Reduction of Fe(acac)₃ by Ascorbic Acid: Role of Water

Ajinkya G. Nene[1]*, Makoto Takahashi[1], Prakash R. Somani[2]

[1]Department of Applied Chemistry, Chubu University, Kasugai, Japan
[2]Applied Science Innovations Pvt. Ltd., Pune, India
Email: *neneajinkya@gmail.com

Abstract

Nanoparticles of Fe₃O₄ and Fe are chemically synthesized by reduction of Fe(acac)₃ using ascorbic acid in controlled condition. It was observed that addition of water during the chemical synthesis process yields Fe₃O₄ nanoparticles, whereas if the reaction is carried out in absence of water yields Fe nanoparticles—which get oxidized upon exposure to air atmosphere. Fe₃O₄ (15 ± 5 nm) and Fe/iron oxide nanoparticles (7 ± 1 nm) were successfully synthesized in the comparative study reported herewith. Mechanism for formation/synthesis of Fe₃O₄ and Fe/iron oxide nanoparticles is proposed herewith in which added water acts as an oxygen supplier. Physico-chemical characterization done by SEM, TEM, EDAX, and XPS supports the proposed mechanism.

Keywords

1. Introduction

Material properties change dramatically in their nano-form as compared to their bulk form [1]. In recent years, magnetic nanoparticles have attracted much attention because of their unique properties and various applications such as in the field of magnetic recording media (e.g. data storage devices, audio and videotape, recording discs, magnetic fluid) [2], various *in vivo* and *in vitro* applications in biomedical science such as cancer hyperthermia, targeted drug delivery, NMR imaging, bioseparation [3]-[5]. Magnetic nanoparticles have applications in catalysis and other industrial usages [4]. Also, magnetic nanoparticles are also used to fabricate nanoscale electronic

---

*Corresponding author.

devices [5].

Magnetite (Fe_3O_4) crystal has an inverse spinel structure with alternating octahedral and tetrahedral sites and shows interesting electrical properties because electrons are transferred between Fe^{2+} and Fe^{3+} ions present in octahedral sites [6]. Main requirement for application of Fe_3O_4 nanoparticles in biomedical science is size less than 20 nm [7]—for their easy penetration and motion inside the human body. In general, as size of Fe_3O_4 nanoparticles decreases the Curie temperature (T_c) also decreases. This puts an additional restriction that Fe_3O_4 nanoparticles should be used below T_c to utilize their magnetic properties. Thus, it is important to select correct size of nanoparticles. At the same time, synthesis method should be highly reproducible, scalable, and economical.

Different polymers and surfactants such as polyvinylalcohol (PVA) [8], poly(vinylpyrolidone) (PVP) [9], polyethylene glycol (PEG) [10], oleic acid [11], polyacrylic acid (PAA) [12] are used for coating of Fe_3O_4 nanoparticles or as capping agent (for controlling the size of the nanoparticles during synthesis and suppressing the aggregration). This results in improved morphology, prevention of agglomeration and aggregation of nanoparticles, but may affect the properties of nanoparticles. Also, polymers and surfactants are expensive and difficult to (naturally) decompose. Thus, their use restricts the applications of Fe_3O_4 nanoparticles in biomedical science and also can cause environmental problems. Fe_3O_4 nanoparticles are prepared by co-precipitation and polyol-methods. There are reports on successful synthesis of Fe_3O_4 nanoparticles by hydrothermal method [13], co-precipitation method [14] [15]. Some of the drawbacks/limitations associated with reported co-precipitation synthesis processes are: slow process and high temperature, size not suitable for *in vivo* biomedical applications (63 ± 25 nm) and wide size distribution [14]. When the magnetite particles (Fe_3O_4) which have a particular stoichiometric composition are made by co-precipitation method, the pH adjustment or pH control is very important and a tedious task. In the coprecipitation method, magnetite nanoparticles are made by the hydrolysis of Fe^{2+} ion and Fe^{3+} ion (mole ratio: 1:2) by a base (usually NaOH or NH_4OH). In this case, overall composition of the precipitate is same as that of the reaction system. But, as the hydrolysis rate of Fe^{3+} ion is greatly different from that of Fe^{2+} ion, the composition of the nanoparticle may not be same. For pH > 11, re-dissolutions of $Fe(OH)_3$ and $Fe(OH)_2$ happen.

$$Fe(OH)_3 \rightarrow Fe(OH)_4^- \qquad Fe(OH)_2 \rightarrow Fe(OH)_3^-$$

There are some other disadvantages of co-precipitation method such as broad nanoparticle size distribution, poor crystallization and irregular crystal shape [16]. Polyol methods need long time (7 - 8 hours) and very high temperature [16]. Exact mechanism leading to formation of Fe_3O_4 and origin of oxygen element in Fe_3O_4 is still unclear in polyol method. Many other methods are reported such as green synthesis methods using plant extracts and bacteria [17] [18], thermal decomposition/pyrolysis of organo-metallic precursors [19]-[22], ultrasound irradiation [23], gamma radiolysis [24], and sol-gel method [25] [26]. Each of these methods has some disadvantages and limitations. Most of these methods yield polydisperse nanoparticles, surface capped nanoparticles, nanoparticles with impurities, in addition to poor reproducibility.

Various methods have been reported for the synthesis of Fe nanoparticles in aqueous medium, but synthesis of Fe nanoparticles by reducing $Fe(acac)_3$ using ascorbic acid is not yet reported. Iron has the highest room temperature saturation magnetization and most importantly its Curie temperature (Tc) is high enough for various possible applications [27]. Fe nanoparticles have various electrical, catalytic, and biomedical applications [27]. In addition, iron is a soft magnetic material with high magnetic moment density [27] [28].

Therefore, it is necessary to develop a simple, cost-effective, reproducible method to synthesize Fe_3O_4 and Fe nanoparticles. In the present study, nanoparticles of Fe_3O_4 and Fe are chemically synthesized by reduction of $Fe(acac)_3$ using ascorbic acid in controlled condition. It was observed that addition of water during the chemical synthesis process yields Fe_3O_4 nanoparticles, whereas if the reaction is carried out in absence of water yields Fe nanoparticles—which were observed to get oxidized upon exposure to air atmosphere while handling (leading to Fe/iron oxide particles). Fe_3O_4 (15 ± 5 nm) and Fe/iron oxide nanoparticles (7 ± 1 nm) were successfully synthesized in the comparative study reported herewith. Mechanism for formation/synthesis of Fe_3O_4 and Fe nanoparticles is proposed based on water as an oxygen supplier [28] [29]. Physico-chemical characterization done by SEM, TEM, EDAX, and XPS supports the proposed mechanism and gives us information about size and shape, polydispersibility, crystallinity and crystal structure, and purity of the material.

2. Experimental

2.1. Chemicals

Chemicals used in this work are: $Fe(acac)_3$ (purity 99%, Strem chemicals, Japan), ascorbic acid (purity 99.6%, Wako Pure Chemicals Industries, Ltd., Japan), dehydrated ethanol (prepared and used when required in our laboratory), diphenyl-ether (purity 99%, Wako Pure Chemicals Industries, Ltd., Japan), and Ultrapure deionized (DI) water. All the chemicals were of analytical grade.

2.2. Instruments

Nanoparticulate powder samples were characterized by X-ray powder diffraction (XRD) using a Rigaku RINT-2100 X-ray diffractometer (Japan) with CuK_α radiation (λ = 1.5406 nm). Transmission electron microscopy (TEM) images were obtained from JEOL JEM-2100F (USA) microscope. X-ray photoelectron spectroscopy (XPS) was done using UlVac Phi Versa Probe CU (Japan).

3. Synthesis of Fe_3O_4 Nanoparticles

In a typical synthesis procedure, 50 mL of 30 mM $Fe(acac)_3$ diphenyl-ether solution was made (by dissolving $Fe(acac)_3$ in diphenyl-ether) and the solution was kept under stirring in N_2 gas atmosphere. Subsequently, temperature was increased up to 70˚C. A reducing acid solution made up of 0.025 M ascorbic acid, 12 M ultrapure water and dehydrated ethanol were then added at a dropping rate of 2 mL/min after the solution temperature reached at 70˚C. After the addition of reducing acid solution, the solution was heated to 190˚C again and refluxed for 1 hour. Finally, it was cooled down to room temperature naturally. Product was separated by filtration and washed 4 - 5 times by chloroform to remove any impurities, followed by dried in vacuum. Dry powder obtained is subsequently used for physico-chemical characterization.

4. Synthesis of Fe Nanoparticles

In another experiment, same procedure (as that for synthesis of Fe_3O_4 nanoparticles) was followed but reducing acid solution made up of dissolving 0.025 M ascorbic acid into dehydrated ethanol (without using ultrapure water) was added at 70˚C with a dropping rate of 2 mL/min.

5. Estimation of Decomposition Efficiency of $Fe(acac)_3$

Same experiment of synthesis reaction was carried out and after the addition of ascorbic acid solution containing dehydrated ethanol, ultrapure water, and ascorbic acid, ultraviolet-visible (UV-VIS) spectrum of 1 mL sample taken at different time interval from reaction and diluted to 50 mL using diphenyl ether was measured to determine the concentration of precursor at that time. The concentration of precursor present in each sample was calculated from absorbance by using Beer-Lamberts law. The decomposition efficiency was calculated by the following equation:

$$\text{Decomposition Efficiency} = \frac{\text{Initial concentration} - \text{Unreacted}}{\text{Initial concentration}} \times 100$$

6. Results and Discussions

Figure 1(a) represents XRD patterns of samples prepared using ultrapure water and without ultrapure water. **Figure 1(a)** shows a typical XRD spectrum of Fe_3O_4 nanoparticles and all peaks can be indexed as pure Fe_3O_4 phase with inverse spinel structure and matched well with the reported data (JCPDS:65-3107). No impurities were detected. The crystallite size calculated by Scherrer equation and full-width-at-half-maximum (FWHM) of the strongest peak (3 1 1) is 15 nm. **Figure 1(b)** shows a comparative study on decomposition efficiency at 70˚C at different ultrapure water concentrations. It can be observable that the change in ultrapure water concentration has no effect on decomposition efficiency. **Figure 1(a)** and **Figure 1(c)** show XRD pattern of samples prepared without using ultrapure water. Peaks at 2θ of 30.22˚, 35.4˚, 43.12˚, 57˚ and 62.84˚ having d values as 2.9558, 2.5338, 2.0966, 1.6145, 1.4776 respectively corresponds to iron oxide. This was expected. This is due to the fact that although sample was prepared in oxygen free condition (in presence of nitrogen); however, sample was
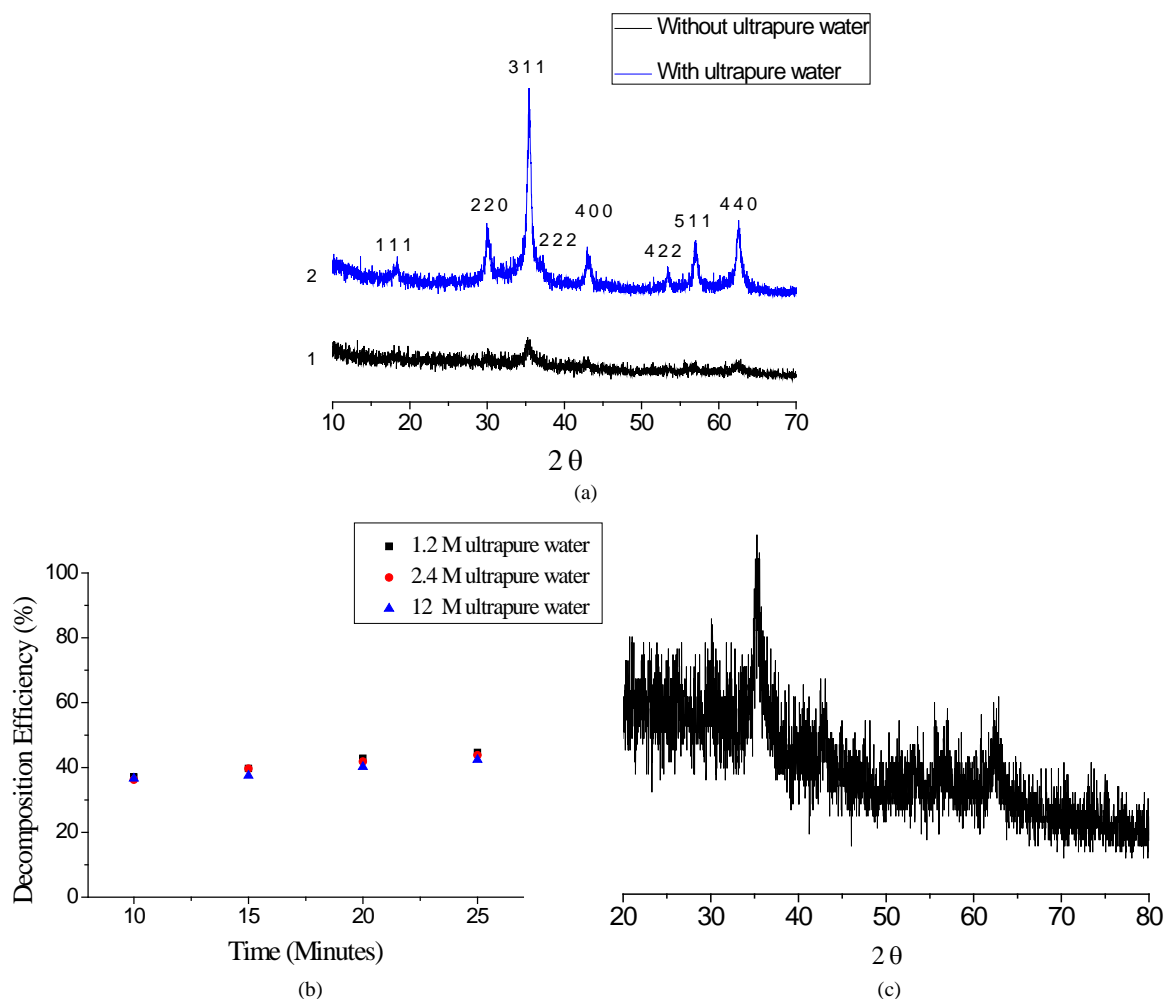
Figure 1. (a) XRD pattern of sample prepared using ultrapure water and without ultrapure water; (b) Decomposition efficiency of Fe(acac)$_3$ at 70˚C at different ultrapure water concentration; (c) XRD pattern of sample prepared without ultrapure water.

exposed to air atmosphere during filtration, drying, and XRD measurement process—leading to formation of iron oxide (Fe/iron oxide nanoparticle). Broad peaks are indicating the amorphous nature of nanoparticles. **Figure 2** represents the EDAX spectra of sample prepared using ultrapure water (a) and without using ultrapure water (b). When ultrapure water was used in reaction then magnetite is formed and EDAX spectrum shows the iron content of 62.16 at% and oxygen of 22.23 at%. Large amount of oxygen is observable in this sample which corresponds to the lattice oxygen (supported by XRD). But when ultrapure water was not used (**Figure 2(b)**) sample shows high content of iron (85.06 at%) and very small amount of oxygen (3.89 at%). We believe that this small amount of oxygen is actually an adsorbed oxygen on the surface of iron nanoparticles when they are exposed to air atmosphere while handling (which is also supported by XRD results). In both the samples, carbon was detected (which is approximately of same amount suggesting our conclusion about oxygen to be true) which arises from carbon tape used for mounting the sample. EDAX measurements were performed at three different locations of each sample and similar results were observed (oxygen of about 3 - 6 at% for the sample prepared without using water, as against 20 - 30 at% for the sample prepared with water).

Figure 3 represents the TEM images of Fe$_3$O$_4$ nanoparticles and Fe/iron oxide nanoparticles, respectively. **Figure 3(a)** represents sample prepared with addition of ascorbic acid solution at 70˚C. The mean particle diameter is observed to be 15 ± 4 nm. Fe$_3$O$_4$ nanoparticles with size less than 25 nm were successfully synthesized by fine tuning of the reaction parameters such as addition temperature, reflux temperature, dropping rate, and reflux time. In **Figure 3(b)**, the size of Fe/iron oxide nanoparticles is observed to be 7 ± 1 nm. Although synthe-
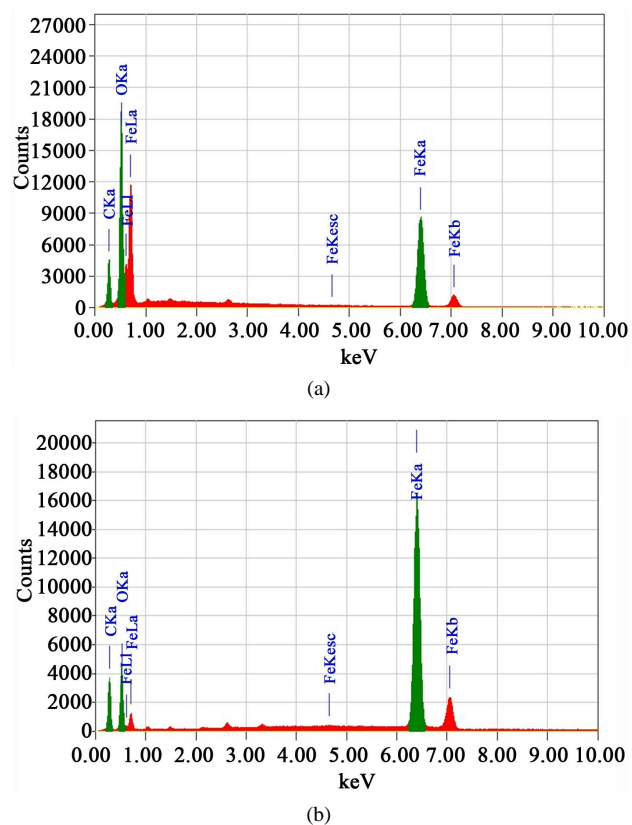
(a)

(b)

Figure 2. EDAX spectra of sample prepared using ultrapure water (a) and without using ultrapure water (b).
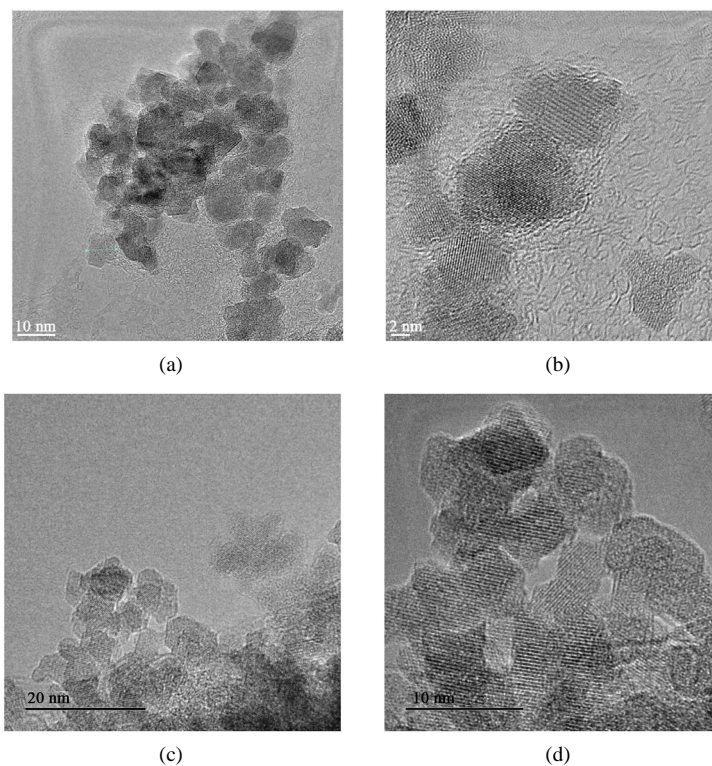

(a)

(b)

(c)

(d)

Figure 3. (a) (b) HRTEM images of Fe_3O_4 nanoparticles; (c) (d) Fe/iron oxide nanoparticles.

sis parameters were same for preparation of both the samples (*i.e.* with and without water); because of the absence of oxygen (coming from water), smaller size Fe/iron oxide nanoparticles have been obtained.

Figure 4 represents XPS spectra of Fe_3O_4 nanoparticles. Sample prepared by using ultrapure water (**Figure 4(a)**) shows Fe2p region which is deconvoluted into 5 peaks. XPS peak at binding energy of 724.70 eV corresponds to $2p_{1/2}$ of Fe^{3+} species, while the peak at binding energy of 722.90 eV can be assigned to 2p1/2 of Fe^{2+} species (in accordance with the earlier reported results) [30]. The peaks at 710.29 eV and 711 eV can be assigned to $2p_{3/2}$ of Fe^{2+} and Fe^{3+} species, respectively [29]. The peak at 719.06 eV is a satellite peak for above four peaks. This shows the formation of Fe_3O_4 nanoparticles.

Fe2p region of sample prepared without ultrapure water (**Figure 4(b)**) is deconvoluted into five peaks. Peak at 707.94 eV correspond to $2p_{3/2}$ of zero-valent iron (Fe^0) confirms the presence of metallic iron [31]-[33]. The peak at 711.21 eV can be assigned to $2p_{3/2}$ of Fe^{3+} species. Photoelectron peaks at 722.93 eV and 724.46 eV can be assigned to $2p_{1/2}$ Fe^{2+} and $2p_{1/2}$ Fe^{3+} species. Peak at 719.02 eV is a satellite peak for all above peaks.

Figure 4(c) and **Figure 4(d)** display the photoelectron spectra of O1s for the sample without using ultrapure water and with ultrapure water, respectively. Both of these spectra show a single broad peak centered around 531 eV and 532 eV, respectively.

No appreciable difference is observable through the XPS analysis between the samples prepared with and without using ultrapure water. This might be due to two reasons: 1) XPS is a surface sensitive technique with very small penetration depth (about 5 nm), and 2) sample prepared without using ultrapure water gets oxidized when exposed to air atmosphere while handling. This was expected due to high reactivity of iron in nanoparticulate form and its affinity and high reactivity towards oxygen. Formation of iron oxide on the surface of iron nanoparticles is also reported earlier by other researchers [29]-[33].
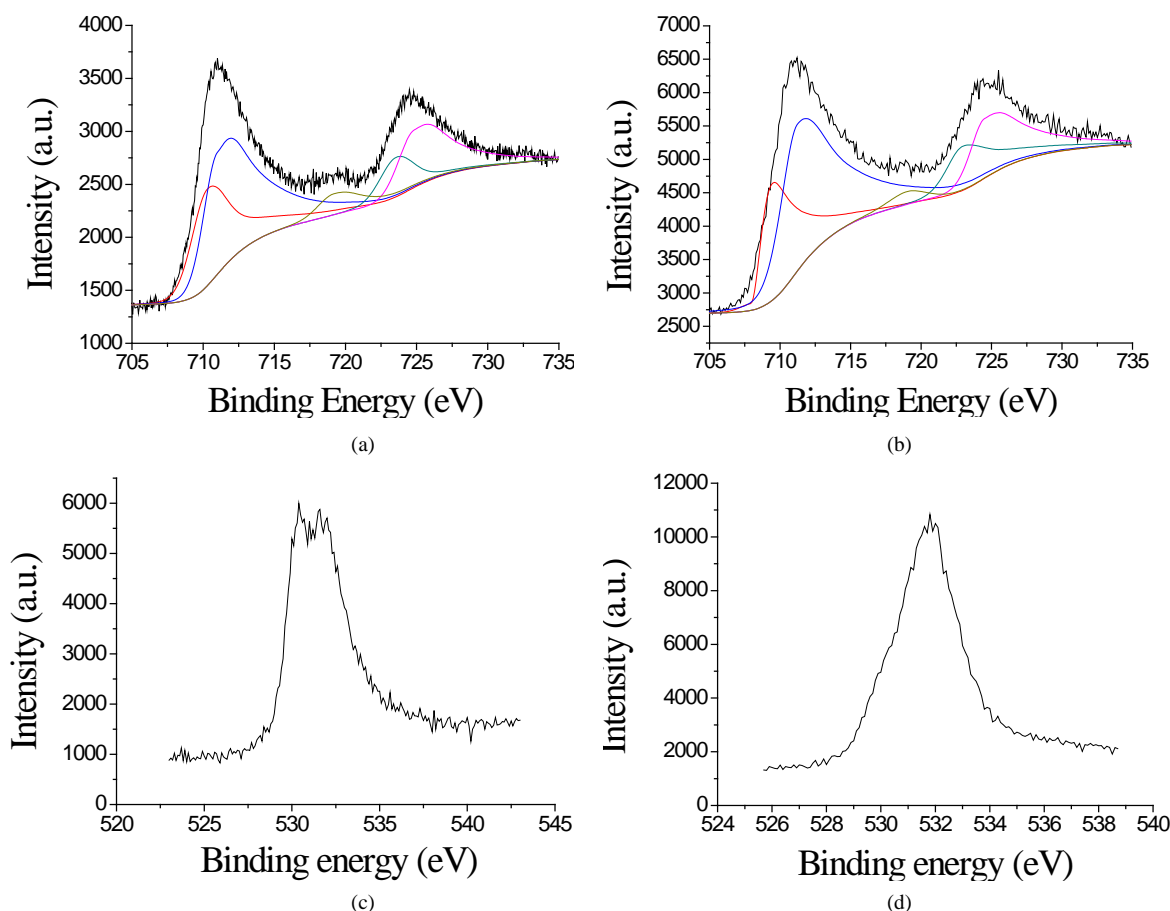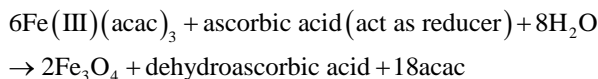

Figure 4. (a) XPS Fe2p spectrum of sample prepared using ultrapure water and (b) without using ultrapure water; (c) O1s spectrum of sample prepared using ultrapure water; (d) O1s spectrum of sample prepared without using ultrapure water.
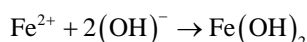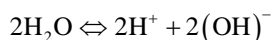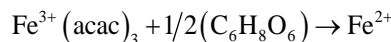
7. Mechanism for Formation of Fe_3O_4 Nanoparticles

In our synthesis process, ascorbic acid acts as reducing agent and ultrapure water acts as supplier of oxygen. The role of dehydrated ethanol is a solvent in ascorbic acid solution. $Fe(acac)_3$ in diphenyl-ether is reduced by ascorbic acid and hydrolyzed by ultrapure water [34].
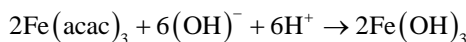
$$6Fe(III)(acac)_3 + \text{ascorbic acid}(\text{act as reducer}) + 8H_2O$$
$$\rightarrow 2Fe_3O_4 + \text{dehydroascorbic acid} + 18acac$$

Ascorbic acid reduces the $Fe(acac)_3$ as follows:

Fe^{2+} is formed because of reduction of $Fe^{3+}(acac)_3$ by ascorbic acid, and because of ultrapure water $Fe(OH)_2$ is generated as follows:

$$Fe^{3+}(acac)_3 + 1/2(C_6H_8O_6) \rightarrow Fe^{2+}$$

$$2H_2O \Leftrightarrow 2H^+ + 2(OH)^-$$

$$Fe^{2+} + 2(OH)^- \rightarrow Fe(OH)_2$$

And $2Fe(OH)_3$ is formed as follows:

$$6H_2O \Leftrightarrow 6H^+ + 6(OH)^-$$

$$2Fe(acac)_3 + 6(OH)^- + 6H^+ \rightarrow 2Fe(OH)_3$$

In general, $Fe(acac)_3$ is reduced by ascorbic acid and $Fe_3(OH)_8$ is synthesized as follows:

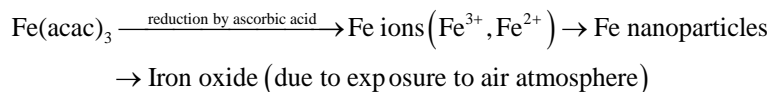$$2Fe^{3+} + Fe^+ + 8H_2O \rightarrow Fe_2^{3+}Fe^{2+}(OH)_8$$
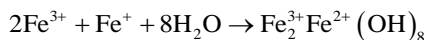
When reaction mixture is heated to reflux, it results in crystallization of Fe_3O_4 nanoparticles and hydrolysis. The formation of Fe_3O_4 is as follows:

$$Fe_3(OH)_8 \xrightarrow{\text{reflux}} Fe_3O_4 + 4H_2O$$
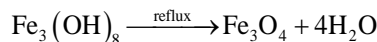
The general reaction can be written as:

$$6Fe(acac)_3 + C_6H_8O_8 + 8H_2O \rightarrow 2Fe_3O_4 + C_6H_6O_6 + 18(acac)$$
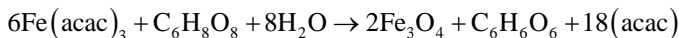
If ultrapure water is not used in reaction, then $Fe(acac)_3$ is reduced by ascorbic acid; but due to lack of oxygen source Fe_3O_4 is not formed, leading to formation of Fe nanoparticles. This also proves that ultrapure water is oxygen supplier in our reaction. In reported polyol-methods, the exact mechanism leading to formation of Fe_3O_4 and origin of oxygen element in Fe_3O_4 is still unclear. Our mechanism proves the origin of oxygen and the role of water during our synthesis process (**Table 1**).

$$Fe(acac)_3 \xrightarrow{\text{reduction by ascorbic acid}} Fe \text{ ions}(Fe^{3+}, Fe^{2+}) \rightarrow Fe \text{ nanoparticles}$$
$$\rightarrow Iron \text{ oxide}(\text{due to exposure to air atmosphere})$$

8. Conclusion

We have successfully developed and demonstrated a new and simple approach to synthesize Fe_3O_4 and Fe nanoparticles (without using any capping agent for size and shape control) in which $Fe(acac)_3$ is reduced by ascorbic acid in a controlled atmosphere with respect to temperature and hydrolyzed by ultrapure water. Ultrapure

Table 1. Elemental composition of samples obtained with and without addition of water during the synthesis process.

Sample	Fe (at%)	O (at%)	C (at%)
Fe_3O_4 (sample with water)	62.16	22.23	15.61
Fe/iron oxide (sample without water)	85.06	3.89	11.05

water acts as oxygen supplier. Fe_3O_4 nanoparticles are observed to form with addition of water; whereas Fe nanoparticles are formed in absence of water. It was observed that such Fe nanoparticles get oxidized to form Fe/iron oxide nanoparticles due to exposure to air atmosphere. Reproducible synthesis of Fe_3O_4 nanoparticles of size 15 ± 5 nm and Fe/iron oxide nanoparticles of size 7 ± 1 nm were achieved. Mechanism for the synthesis of Fe_3O_4 and Fe nanoparticles is proposed. Method presented herewith should prove to be very useful for synthesis of Fe_3O_4 nanoparticles having surface available for further use such as uploading of drug molecules for biomedical applications. Further work for biomedical application of these nanoparticles is in progress.

Acknowledgements

References

[1] Yang, T., Shen, C., Yang, H., Xiao, C., Xu, Z., Chen, S., Shi, D. and Gao, H. (2006) Synthesis, Characterization and Self-Assemblies of Magnetite Nanoparticle. *Surface and Interface Analysis*, **38**, 1063-1067. http://dx.doi.org/10.1002/sia.2329

[2] Ghandoor, H., Zidan, H., Khalil, M. and Ismail, M. (2012) Synthesis and Some Physical Properties of Magnetite (Fe_3O_4) Nanoparticles. *International Journal of Electrochemical Science*, **7**, 5734-5745.

[3] Akbarzadeh, A., Samiei, M. and Davaran, S. (2012) Magnetic Nanoparticles: Preparation, Physical Properties, and Applications in Biomedicines. *Nanoscale Research Letters*, **7**, 144. http://dx.doi.org/10.1186/1556-276X-7-144

[4] Durdureanu-Angheluta, A., Pinteala, M. and Simionescu, B.C. (2012) Tailored and Functionalized Magnetic Particles for Biomedical and Industrial Applications. In: Hutagalung S.D., Ed., *Material Science and Technology*, In Tech, Rijeka (Croatia), 149-178. http://dx.doi.org/10.5772/30217

[5] Singamaneni, S., Bliznyuk, V., Binek, C. and Tsymbal, E. (2011) Magnetic Nanoparticles: Recent Advances in Synthesis, Self-Assembly and Applications. *Journal of Materials Chemistry*, **21**, 16819-16845. http://dx.doi.org/10.1039/c1jm11845e

[6] Blaney, L. (2007) Magnetite (Fe_3O_4): Properties, Synthesis and Applications. *The Lehigh Review*, **15**, 33.

[7] Sun, S. and Zeng, H. (2002) Size-Controlled Synthesis of Magnetite Nanoparticles. *Journal of the American Chemical Society*, **124**, 8204-8205. http://dx.doi.org/10.1021/ja026501x

[8] Kurchania, R., Sawant, S. and Ball, R. (2014) Synthesis and Characterization of Magnetite/Polyvinyl Alcohol Core-Shell Composite Nanoparticles. *Journal of the American Chemical Society*, **97**, 3208-3215. http://dx.doi.org/10.1111/jace.13108

[9] Lu, X., Niu, M., Qiao, R. and Gao, M. (2008) Superdispersible PVP-Coated Fe_3O_4 Nanocrystals Prepared by a "One-Pot" Reaction. *Journal of Physical Chemistry B*, **112**, 14390-14394. http://dx.doi.org/10.1021/jp8025072

[10] Mukhopadhyay, A., Joshi, N., Chattopadhyay, K. and De, G. (2012) A Facile Synthesis of PEG-Coated Magnetite (Fe_3O_4) Nanoparticles and Their Prevention of the Reduction of Cytochrome C. *Applied Materials & Interfaces*, **4**, 142-149. http://dx.doi.org/10.1021/am201166m

[11] Zhang, L., He, R. and Gu, H. (2006) Oleic Acid Coating on the Monodisperse Magnetite Nanoparticles. *Applied Surface Science*, **253**, 2611-2617. http://dx.doi.org/10.1016/j.apsusc.2006.05.023

[12] Zhou, C., Zhang, W., Xia, M., Zhou, W., Wan, Q., Peng, K. and Zou, B. (2013) Synthesis of Poly(acrylic acid) Coated-Fe_3O_4 Superparamagnetic Nano-Composites and Their Fast Removal of Dye from Aqueous Solution. *Journal of Nanoscience and Nanotechnology*, **13**, 4627-4633. http://dx.doi.org/10.1166/jnn.2013.6886

[13] Daou, T., Pourroy, G., Colin, S., Greneche, J., Bouillet, C., Legare, P., Bernhardt, P., Leuvrey, C. and Rogez, G. (2006) Hydrothermal Synthesis of Monodisperse Magnetite Nanoparticles. *Chemistry of Materials*, **18**, 4399-4404. http://dx.doi.org/10.1021/cm060805r

[14] Mascolo, M., Pei, Y. and Ring, T. (2013) Room Temperature Co-Precipitation Synthesis of Magnetite Nanoparticles in a Large pH Window with Different Bases. *Materials*, **6**, 5549-5567. http://dx.doi.org/10.3390/ma6125549

[15] Lopez, J., Gonzalez, F., Bonilla, F., Zambrano, G. and Gomez, M. (2010) Synthesis and Characterization of Fe_3O_4 Magnetic Nanofluid. *Revista Latinoamericana de Metalurgia y Materiales*, **30**, 60-66.

[16] Das, M., Dhak, P., Gupta, S., Mishra, D., Maiti, T., Basak, A. and Pramanik, P. (2010) Highly Biocompatible and Water Dispersible Amine Functionalized Magnetite Nanoparticles, Prepared by a Low Temperature, Air Assisted Polyol

Process: A New Platform for Bio-Separation and Diagnostics. *Nanotechnology*, **21**, Article ID: 125103. http://dx.doi.org/10.1088/0957-4484/21/12/125103

[17] Senthil, M. and Ramesh, C. (2012) Biogenic Synthesis of Fe_3O_4 Nanoparticles Using *Tridax Procumbens* Leaf Extract and Its Antibacterial Activity on *Pseudomonas aeroginosa*. *Digest Journal of Nanomaterials & Biostructures*, **7**, 1655-1660.

[18] Alagu Sundaram, P., Augustine, R. and Kannan, M. (2012) Extracellular Biosynthesis of Iron Oxide Nanoparticles by *Bacillus subtilis* Strains Isolated from Rhizosphere Soil. *Biotechnology and Bioprocess Engineering*, **17**, 835-840. http://dx.doi.org/10.1007/s12257-011-0582-9

[19] Angermann, A. and Topfer, J. (2008) Synthesis of Magnetite Nanoparticles by Thermal Decomposition of Ferrous Oxalate Dehydrate. *Journal of Materials Science*, **43**, 5123-5130. http://dx.doi.org/10.1007/s10853-008-2738-3

[20] Zhao, F., Zhang, B. and Feng, L. (2012) Preparation and Magnetic Properties of Magnetite Nanoparticles. *Materials Letters*, **68**, 112-114. http://dx.doi.org/10.1016/j.matlet.2011.09.116

[21] Shi, R.R., Gao, G.H., Yi, R., Zhou, K.C., Qiu, G.Z. and Liu, X.H. (2009) Controlled Synthesis and Characterization of Monodisperse Fe_3O_4 Nanoparticles. *Chinese Journal of Chemistry*, **27**, 739-744. http://dx.doi.org/10.1002/cjoc.200990122

[22] Wang, L. and Jiang, J. (2009) Preparation of Fe_3O_4 Spherical Nanoporous Particles Facilitated by Polyethylene Glycol 4000. *Nanoscale Research Letters*, **4**, 1439. http://dx.doi.org/10.1007/s11671-009-9417-4

[23] Qiu, G., Wang, Q. and Nie, M. (2006) Polypyrrole-Fe_3O_4 Magnetic Nanocomposite Prepared by Ultrasonic Irradiation. *Macromolecular Materials and Engineering*, **291**, 68-74. http://dx.doi.org/10.1002/mame.200500285

[24] Abedini, A., Daud, A.R., Abdul Hamid, M.A. and Kamil Othman, N. (2014) Radiolytic Formation of Fe_3O_4 Nanoparticles: Influence of Radiation Dose on Structure and Magnetic Properties. *PLoS ONE*, **9**, e90055. http://dx.doi.org/10.1371/journal.pone.0090055

[25] Xu, J., Yang, H., Fu, W., Du, K., Sui, Y., Chen, J., Zeng, Y., Li, M. and Zou, G. (2007) Preparation and Magnetic Properties of Magnetite Nanoparticles by Sol-Gel Method. *Journal of Magnetism and Magnetic Materials*, **309**, 307-311. http://dx.doi.org/10.1016/j.jmmm.2006.07.037

[26] Lemine, O., Omri, K., Zhang, B., El Mirb, L., Sajieddine, M., Alyamani, A. and Bououdina, M. (2012) Sol-Gel Synthesis of 8 nm Magnetite (Fe_3O_4) Nanoparticles and Their Magnetic Properties. *Superlattices and Microstructures*, **52**, 793-799. http://dx.doi.org/10.1016/j.spmi.2012.07.009

[27] Huber, D. (2005) Synthesis, Properties, and Applications of Iron Nanoparticles. *Small*, **1**, 482-501. http://dx.doi.org/10.1002/smll.200500006

[28] Peng, S., Wang, C., Xie, J. and Sun, S. (2006) Synthesis and Stabilization of Monodisperse Fe Nanoparticles. *Journal of the American Chemical Society*, **128**, 10676-10677. http://dx.doi.org/10.1021/ja063969h

[29] Prabu, D. and Parthiban, R. (2013) Synthesis and Characterization of Nanoscale Zero Valent Iron (NZVI) Nanoparticles for Environmental Remediation. *Asian Journal of Pharmaceutical Technology*, **3**, 181-184.

[30] Martinez, G., Malumbres, A., Mallada, R., Hueso, J., Irusta, S., Bomati-Miguel, O. and Santamaria, J. (2012) Use of a Polyol Liquid Collection Medium to Obtain Ultrasmall Magnetic Nanoparticles by Laser Pyrolysis. *Nanotechnology*, **23**, Article ID: 425605. http://dx.doi.org/10.1088/0957-4484/23/42/425605

[31] Sun, Y.P., Li, X.Q., Zhang, W.X. and Wang, H.P. (2007) A Method for the Preparation of Stable Dispersion of Zero-Valent Iron Nanoparticles. *Colloids and Surfaces A*: *Physicochemical and Engineering Aspects*, **308**, 60-66. http://dx.doi.org/10.1016/j.colsurfa.2007.05.029

[32] Sun, Y., Li, X., Cao, J., Zhang, W. and Wang, H. (2006) Characterization of Zero-Valent Iron Nanoparticles. *Advances in Colloid and Interface Science*, **120**, 47-56. http://dx.doi.org/10.1016/j.cis.2006.03.001

[33] Watson, S., Mohamed, H., Horrocksa, B. and Houlton, A. (2013) Electrically Conductive Magnetic Nanowires Using an Electrochemical DNA-Templating Route. *Nanoscale*, **5**, 5349-5359. http://dx.doi.org/10.1039/c3nr00716b

[34] Nene, A.G., Takahashi, M., Somani, P.R., Aryal, H., Wakita, K. and Umeno, M. (2016) Synthesis and Characterization of Graphene-Fe_3O_4 Nanocomposite. *Carbon—Science and Technology*, **8**, 13-24.